Fifty-third Annual Allerton Conference
Allerton House, UIUC, Illinois, USA
September 29 - October 2, 2015

Enabling renewable resource integration: The balance between robustness and flexibility

Gabriela Martínez, Jialin Liu, Bowen Li, Johanna L. Mathieu, and C. Lindsay Anderson

***Abstract*— The steady rise of electricity demand and renewable energy sources is increasing the need for flexibility to enable power systems to adapt to changes in supply and demand. To this end, demand response programs have the potential to increase the flexibility of the system. In this work, a direct-load-control demand response program is used in the scheduling task of a power system with high levels of variable renewable generation. The model considers different classes of reserves provided by both conventional generation and responsive demand. Unit commitment, generator dispatch and reserve allocations are determined with appropriate risk-averse levels to guarantee a reliable and feasible operation of the system across the planning horizon. Risk preferences are reflected in constraint satisfaction via robust and probabilistically-constrained approaches. Case studies with a 57-bus system show that the probabilistic approach allows higher wind share in the power network and incurs lower costs than the robust approach. In addition, results show that controllable loads are an important contributor to system flexibility, though addition of other classes of responsive demand will also bring desirable flexibility.**

I. Introduction

As power systems shift to integrate higher levels of uncertain renewable resources, updated operational processes are required to improve the flexibility and maintain the reliability of the power system. In this regard, demand response (DR) programs, defined by the Department of Energy as "electricity tariff or program established to motivate changes in electric use by end-use customers, designed to induce lower electricity use at times of high market prices or when system reliability is jeopardized" [1], can play an active role in improving the flexibility of the system as well as strengthening its reliability [2], [3].

In 2015, wind penetration is reaching new levels globally, with the U.S. system obtaining nearly 10% of total energy from this environmentally benign, but intermittent, resource. As the utilization of wind resources continues to increase, the power system will require methods to incorporate uncertainty and to leverage any available flexibility to operate in an efficient and reliable manner [4]–[6]. Included in potential sources of flexibility are the use of demand side resources, in the form of responsive loads. These loads can be roughly categorized as price-based demand response, in which users respond to price signals, and incentive-based demand response, typically managed by aggregators or load-serving entities [7].

Demand response programs are not new, for example, incentive programs designed to reduce load consumption can be traced back to 1970 in the U.S.. Previous research has shown several potential benefits of DR, including peak-load reduction, mitigation of outage risk, market-clearing price reduction, and improving social welfare [1], [8]–[11]. The flexibility provided by DR offers attractive opportunities to meet fluctuations of renewable generation, for example, the effects of participation of price-based DR in the electricity market and its impacts on unit commitment (UC) for a system with variable generation is analyzed in [12]. The study presented in [13] shows that price-based DR can mitigate the cost effects of wind generation in UC decision processes, and the simulation analysis performed in [14] illustrates the effects of price-based DR in UC decisions for power systems with wind and solar photovoltaic (PV) power. Recent studies have focused on developing stochastic optimization approaches for UC decisions of power systems with renewable energy and DR. In [15] a stochastic two-stage UC model with a price-based demand response program is used to show the benefits of coupling deferrable loads with renewable energy. In [16] a stochastic two-stage incentive-based demand response model is used to determine a load shifting schedule to maximize the expected usage of the power produced by PV panels. Robust optimization approaches have also been proposed in the literature. For example, in [17] a robust optimization model is used to determine UC decisions under the joint worst-case wind power output and price-based demand response scenario. A robust $n-k$ contingency UC model, which uses the worst-case price-based demand response scenario to attenuate the impact of multiple contingencies in a power system, is developed in [18].

In this work, an incentive-based DR program exploits the potential of thermostatically controlled loads (TCLs), such as heating, air conditioners, and refrigerators, to provide reserve capacity to the system. The the chance-constrained optimal power flow (CC-OPF) model presented in [19]–[21] is extended to include the unit commitment (UC) problem and generator ramping constraints. A scheduling task is implemented to determine an optimal allocation of generating and load reserves in response to variations of renewable energy production. This approach adjusts the risk-level tolerance of the system to provide greater flexibility to the system in order to accommodate sudden variations of renewable energy production at each period of time of the

G. Martínez, J. Liu, and C.L. Anderson are with Cornell University, {mgm256,jl3455,cla28}@cornell.edu. B. Li and J.L. Mathieu are with the University of Michigan, {libowen,jlmath}@umich.edu. This work was supported in part by the Consortium for Electric Reliability Technology Solutions and the Office of Electricity Delivery and Energy Reliability, Transmission Reliability Program of the U.S. Department of Energy, and the National Science Foundation Grants #CCF-1442495 and #ECCS-1453615.

978-1-5090-1824-6/15/$31.00 ©2015 IEEE

planning horizon. The simulation study considers the impact of different risk levels, and responsive load on the efficacy of wind integration in the system.

The structure of the paper is as follows; an overview of the the demand response model and the chance-constrained scheduling task of the system are presented in Section II. Numerical experiments are reported in Section III, and concluding remarks and future directions are detailed in Section IV.

II. Model Formulation

In this section, the structure of the unit commitment model is described, which is based on the stochastic optimal power flow model developed in [19], [20], with the following modifications: 1) the daily temperature profile is deterministic, which makes the capacity of the load reserve deterministic; 2) conservative coupling constraints are deleted to reduce computational complexity; 3) wind capacity is increased and dispersed among four wind farms on the network using realistic forecast and error characteristics; and 4) binary commitment variables and generator ramping limits are added to the economic dispatch problem in [19], [20] to include the unit commitment problem in the framework.

A. Nomenclature

$\mathcal{C}^{\text{det}}$	deterministic constraints on generators, flows, loads, and storage
$\mathcal{C}_{GD}$	probabilistic constraints associated with the re-dispatch reserves from generators
$\mathcal{C}_{GS}$	probabilistic constraints associated with the secondary reserves from generators
$\mathcal{C}_{LS}$	probabilistic constraints associated with the secondary reserves from controllable loads
$\delta\tau$	time step length
ϵ	constraint violation probability
$\mathcal{T}$	ambient temperature
$\overline{R}_g$	generator upper ramp rate limit vector
$\underline{R}_g$	generator lower ramp rate limit vector
A	matrix that maps power injections to line flows
C_G	matrix that maps generator injections to buses
C_L	matrix that maps load consumption to buses
C_n	cost function of the generators
C_W	matrix that maps wind injections to buses
C_{gd}	cost function of the re-dispatch reserves from generators
C_{gs}	cost function of the secondary reserves from generators
C_{ls}	cost function of the secondary reserves from controllable loads
$d_{gd}^{1,up/dn}$	generator upward/downward re-dispatch reserve distribution vector for restoring generators/loads to scheduled power dispatch
$d_{gd}^{2,up/dn}$	generator upward/downward re-dispatch reserve distribution vector for restoring controllable load to scheduled energy state
$d_{gs}^{up/dn}$	generator upward/downward secondary reserve distribution vector
$d_{ls}^{up/dn}$	controllable load upward/downward secondary reserve distribution vector
DT_g	generator minimum down time
k_g	minimum generation cost
N_b	number of buses
N_t	number of periods
P_b	controllable load baseline power vector
P_c^+	controllable load power upper bound vector
P_c^-	controllable load power lower bound vector
P_g^+	generator generation upper bound vector
P_g^-	generator generation lower bound vector
P_c	controllable load power set point vector
P_g	generator generation vector
P_{inj}	bus power injection vector
P_{line}	line limit vector
P_l	non-controllable load power vector
P_w^f	forecasted wind power vector
$R_{gd}^{up/dn}$	generator upward/downward re-dispatch reserve capacity vector
$R_{gs}^{up/dn}$	generator upward/downward secondary reserve capacity vector
$R_{ls}^{up/dn}$	controllable load upward/downward secondary reserve capacity vector
S	controllable load energy state vector
S^+	controllable load energy state upper bound vector
s_g	generator start-up cost
t	time index
UT_g	generator minimum up time
w_g	generator commitment binary variable
z_g	generator binary start-up variable

B. Demand Response Model

The demand response model uses an aggregation of TCLs to provide reserve resources to the system. As detailed in [22], aggregations of these loads are modeled as thermal energy storage that exhibit time varying power and energy capacities as a function of ambient temperature $\mathcal{T}_t$. TCLs are used to provide flexibility to the system by manipulating their power consumption while ensuring that the temperatures they are modulating remain within narrow temperature bands (e.g., 1°C) around their temperature set points. To ensure that the TCL temperatures stay within these bands, energy capacity bounds $[0, S^+(\mathcal{T}_t)]$ and power capacity bounds $[P_c^-(\mathcal{T}_t), P_c^+(\mathcal{T}_t)]$ are applied to the energy state S_t and power state $P_{c,t}$ of the controllable load across all time periods as follows:

$$0 \leq S_t \leq S^+(\mathcal{T}_t) \tag{1}$$

$$P_c^-(\mathcal{T}_t) \leq P_{c,t} \leq P_c^+(\mathcal{T}_t) \tag{2}$$

Additionally, the energy state evolves as

$$S_{t+\delta\tau} = S_t + (P_{c,t} - P_b(\mathcal{T}_t))\delta\tau \tag{3}$$

where $P_b(\mathcal{T}_t)$ is the baseline power consumption of the load aggregation and $\delta\tau$ is the length of each time step. Methods of calculating the power and energy capacity associated with aggregations of TCLs are described in [22]. Here, we use an

aggregation of air conditioners, and use the power and energy capacity profiles from [21].

C. Day-ahead Unit Commitment Model

The goal of the day-ahead unit commitment is to compute the generation schedule P_g, the controllable load schedule P_c, the generator commitment binary vector w_g, and the generator start-up binary vector z_g. Additionally, in this model there are three classes of reserves: secondary reserve from generators R_{gs} (with capacity $R_{gs}^{up/dn}$, where up and dn denote up-reserves and down-reserves), secondary reserve from loads R_{ls} (with capacity $R_{ls}^{up/dn}$), and re-dispatch reserve R_{gd} (with capacity $R_{gd}^{up/dn}$) from generators. Both types of secondary reserve are used to manage deviations between forecasted and realized wind generation. The secondary generator reserve distribution vectors $d_{gs}^{up/dn}$ and load reserve distribution vector $d_{ls}^{up/dn}$ distribute wind deviations to individual generators. The re-dispatch reserve is activated every 15 minutes and has two functions; first, to make up for the intra-hour wind forecast error, and second, to provide energy to bring the loads back to their scheduled energy state. Those two functions are accounted for by the distribution vectors $d_{gd}^{1,up/dn}$ and $d_{gd}^{2,up/dn}$, respectively. The optimization variables are denoted by the vector x_t, and include:

$$\begin{aligned} x_t = [&w_{g,t}, z_{g,t}, P_{g,t}, P_{c,t}, R_{gs,t}^{up}, R_{gs,t}^{dn}, R_{ls,t}^{up}, R_{ls,t}^{dn}, \\ &R_{gd,t}^{up}, R_{gd,t}^{dn}, d_{gs,t}^{up}, d_{gs,t}^{dn}, d_{ls,t}^{up}, d_{ls,t}^{dn}, d_{gd,t}^{1,up}, \\ &d_{gd,t}^{1,dn}, d_{gd,t}^{2,up}, d_{gd,t}^{2,dn}]. \end{aligned}$$

The objective function of the model is defined as

$$\begin{aligned} F(\{x_t\}_{t=1}^T) &= \textstyle\sum_{t=1}^T (k_g w_{g,t} + s_g z_{g,t} \\ &+ C_n(P_{g,t}) + C_{gs}(R_{gs,t}^{up/dn}) \\ &+ C_{ls}(R_{ls,t}^{up/dn}) + C_{gd}(R_{gd,t}^{up/dn})), \end{aligned}$$

where k_g is the minimum generation cost, s_g is the generator start-up cost, and each C represents a convex, increasing cost function.

The deterministic constraints $\mathcal{C}^{\text{det}}$ are with respect to 24-hour wind forecast P_w^f and are listed below. For $t \in \{1, ..., T\}$:

$$\mathbf{1}_{1\times N_b} P_{inj,t} = 0 \tag{4}$$

$$-P_{line} \le A P_{inj,t} \le P_{line} \tag{5}$$

$$P_g^- w_{g,t} \le P_{g,t} \le P_g^+ w_{g,t} \tag{6}$$

$$\underline{R}_g \le P_{g,t} - P_{g,t+1} \le \overline{R}_g \tag{7}$$

$$z_{g,t} = w_{g,t} - w_{g,t-1} \tag{8}$$

$$\sum_{q=t-UT_g+1}^{t} z_{g,q} \le w_{g,t-1}, \quad \text{if } UT_g \le t \tag{9}$$

$$\sum_{q=t+1}^{t+DT_g} z_{g,q} \le 1 - w_{g,t-1}, \quad \text{if } |T| - DT_g \le t \tag{10}$$

along with (1)–(3) and

$$0 \le S_{t+1} \le S^+(\mathcal{T}_t) \tag{11}$$

where UT_g and DT_g are the minimum up and down time of the generators; P_g^- and P_g^+ are the generator generation limits; and $\underline{R}_g$ and $\overline{R}_g$ are the generator ramp rate limits. The matrix A maps the power injections to the line flows; the derivation is in [23]. The line flows are bounded by P_{line}. $P_{inj,t}$ is the DC net power injection of buses at time $t \in \{1, ..., T\}$:

$$P_{inj,t} = C_G P_{g,t} + C_W P_{w,t}^f - C_L(P_{l,t} + P_{c,t}),$$

where the matrices C_G, C_W, C_L map the generator, wind and load power injections to the corresponding buses. Please refer to [23] for the details of this power flow formulation.

Additional model constraints are classified as secondary reserve load constraints $\mathcal{C}_{LS}$, secondary reserve generator constraints $\mathcal{C}_{GS}$, and generator re-dispatch constraints $\mathcal{C}_{GD}$, all of which are impacted by the stochastic wind forecast error and are therefore modeled as stochastic constraints. Details of all classes of constraints are provided in [23]. In brief, $\mathcal{C}_{LS}$ and $\mathcal{C}_{GS}$ include stochastic versions of the deterministic power flow constraints, generation and load constraints that include the impact of secondary reserve actions, and reserve constraints that allow generators/loads to compensate for wind power error. Similarly, $\mathcal{C}_{GD}$ includes generation and load limits that include the impact of re-dispatch actions, and reserve limits that allow generators to compensate for intra-hour wind error and reset loads to their schedules.

Finally, the optimal day-ahead dispatch can be formulated as:

$$\begin{aligned} \text{minimize}_{\{x_t\}_{t=1}^T} \; & F\left(\{x_t\}_{t=1}^T\right) \\ \text{subject to} \; & \mathcal{C}^{\text{det}} \\ & \mathbb{P}\left(\mathcal{C}_{LS} \cap \mathcal{C}_{GS} \cap \mathcal{C}_{GD}\right) \ge 1 - \epsilon \end{aligned}$$

where the stochastic constraints are required to be met jointly at a probability level of $1 - \epsilon$. The operator could also set different probability levels for different constraints at different times according to their relative importance. The introduction of binary commitment variables in this formulation is handled through a first-stage deterministic optimization for commitments based on wind forecasts, and the stochasticity of forecast errors are managed in the second stage of the CC-OPF with reserves.

III. Numerical Results

In this section, the test setting first described, followed by case study results considering the impact of controllable loads at different risk levels.

A. Test Setting

The model described is implemented on the IEEE 57-bus system, which is augmented with addition of four wind farms located at buses 1, 10, 20, and 57. The data of the system can be found in [24, case57]. In these simulations, the total air conditioning load is a function of the ambient temperature, which is represented by a representative summer day in New York City. To determine the capacity of load that is

controllable, a specific percentage (10% or 20%) of the total air conditioning load is used.

The wind data for each wind farm is selected from the NREL-Eastern Wind Integration Study dataset [25], located to reasonably match the location of the temperature data. Using three years of data, 24-hour trajectories are clustered to identify a set of similar trajectories, with a common initial state. The largest set contained 54 trajectories and were used to represent the realizations of a similar forecast. The central trajectory of the cluster was selected as the wind forecast, and the remaining were used to estimate the distribution of forecast errors, as described in [26]. From the forecast error distribution, 10000 scenarios are used to generate a robust wind error scenario set. The maximum share of wind power (WS) in our study goes up to 30% of the total system load.

Table I gives the cost of different reserves. The upward and downward reserves are assumed to have the same cost. The cost of the secondary generator reserves is higher than that of the re-dispatch reserves as the secondary reserves respond faster. The cost of the load reserve is

$$C_{ls,t} = 1.1 - \tilde{S}(\mathcal{T}_t), \tag{13}$$

where $\tilde{S}(\mathcal{T}_t)$ is normalized by the maximum hourly load energy bound, and, again, the upward and downward reserves are assumed to have the same cost.

TABLE I: Generator Reserve Costs

Generator	1	2	3	4	5	6	7
C_{gs}	51	101	70	98	52	103	47
C_{gd}	31	52	40	50	29	49	30

Two approaches are used in our model: the robust approach developed by [27] and the percentile approach developed by [28]. The robust approach considers the worst case scenario of the wind forecast, whereas the percentile approach gives the system operators the flexibility to set the risk level to satisfy a certain percentage of the possible scenarios.

The problem is implemented in MATLAB and solved by the optimization package Gurobi solver Version 6.0.4.

B. Results

The objective of this study is to analyze the impact of flexibility in achieving significant wind integration targets. To this end, we first summarize the overall feasibility of the system solution with increasing wind share. These results are summarized in Table II, where 'I' and 'F' indicate 'Infeasible' and 'Feasible' solutions, respectively.

TABLE II: Feasibility (F) and Infeasibility (I) of robust and percentile ($\epsilon = 0.05$) solutions with increasing wind capacity and 10% controllable load or no controllable load

WS	10%	15%	20%	25%	30%
Robust	F	F	I	I	I
Percentile (10% CL)	F	F	F	F	F
Percentile (0% CL)	F	F	F	F	I

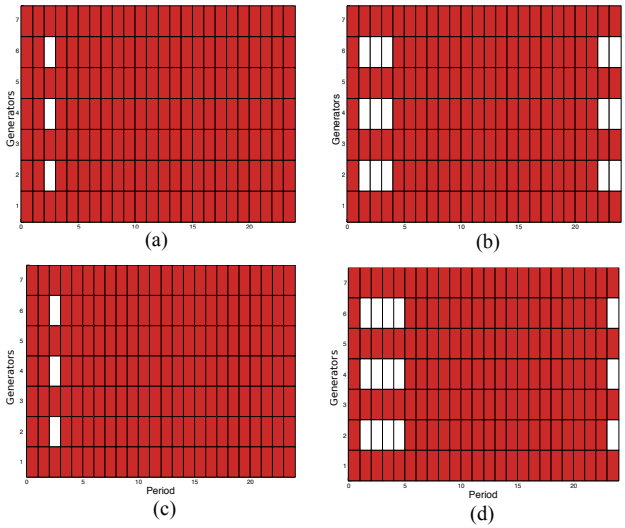

Fig. 1: Committed Units (red), with 15% Wind Penetration: Robust solution (a) 10% CL, (b) 20% CL, and Probabilistic solution ($\epsilon = 0.05$) (c) 10% CL, (d) 20% CL

The results shown in Table II show that, while the robust solution provides the most reliable allocations of generation and reserves, the demands placed on the generation units are such that so feasible solution exists for wind levels over 15%. Conversely, the increased flexibility of the probabilistic approach appears sufficient to incorporate the higher proportions of variable resources, which is enabled at by the availability of reserves from controllable load (CL). Interestingly, increasing levels of controllable to 20% does not impact feasibility results for robust solutions.

Next, the unit commitment solutions are considered for various combinations of wind penetration and controllable load. Figure 1 shows the committed units for 15% wind share, with both robust and probabilistic approaches, while Fig. 2 shows the committed units for 30% wind with both 10% and 20% controllable loads. It should also be noted that in all cases, when no controllable load is available, all units are committed in both the robust and probabilistic cases, regardless of wind share, and that no commitment schedule exists that can ensure a robust solution with 30% wind. Figures 1 and 2 show that flexibility in risk levels, and the added flexibility from controllable loads are likely to be important contributors in the ability to integrate the uncertain and variable renewables.

In addition to the homogeneously robust and percentile approaches, a hybrid approach is explored, which uses adjustable percentiles based on the characteristics of the wind forecast error. Specifically, forecasting the day ahead wind generation is always more accurate during earlier hours of forecast, and increases as the forecast horizon increases [29]. An empirical plot of typical root mean square (RMS) forecast error is shown in Fig. 3, and Fig. 4 shows the wind forecast and scenarios for 20% wind share. In this case, it may be valuable to use a more risk-averse solution method as the forecast becomes less accurate.

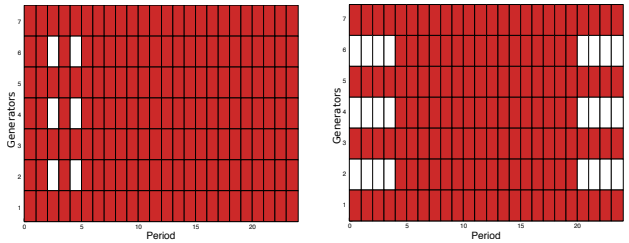

(a) (b)

Fig. 2: Committed Units (red), with 30% Wind Penetration: Probabilistic solution ($\epsilon = 0.05$) (a) 10% CL, (b) 20% CL

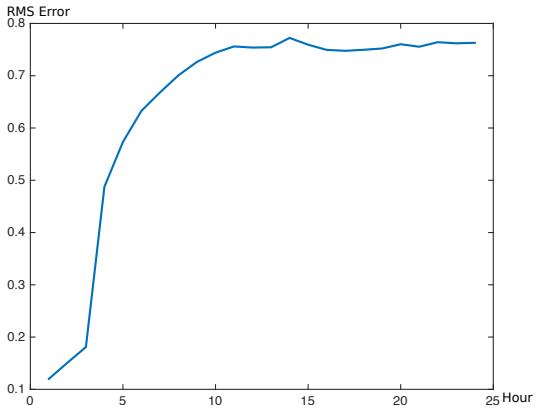

Fig. 3: Wind RMS forecast error over one day.

In the following results, this 'mixed' approach is also considered, wherein a probabilistic approach is used in the early hours of the day (hours zero through nine), and robust approach is used for the remaining hours. This selection is based on the RMS error threshold of 0.7, but could be customized to the operator preferences and specific forecast characteristics. In Fig. 5 the upward and downward reserves allocated for 15% wind share, with controllable loads, is provided for robust, probabilistic and mixed approach, respectively.

The reserve allocations shown in Fig. 5 show that while the load reserves are fairly similar across risk-levels, the

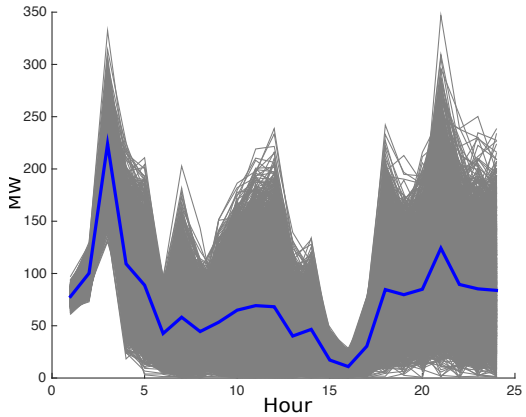

Fig. 4: Aggregated wind power forecast (blue) and scenarios (grey).

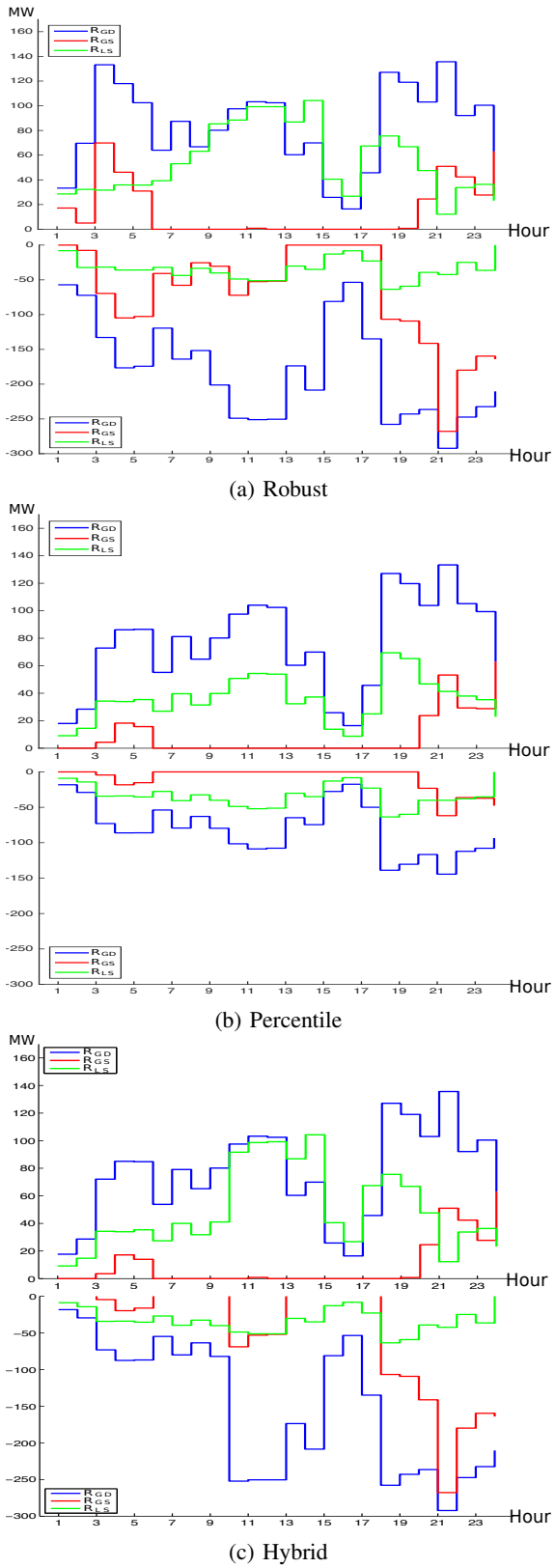

(a) Robust

(b) Percentile

(c) Hybrid

Fig. 5: Reserve allocations for loads (green), generator secondary (red), and generator re-dispatch (blue) reserves

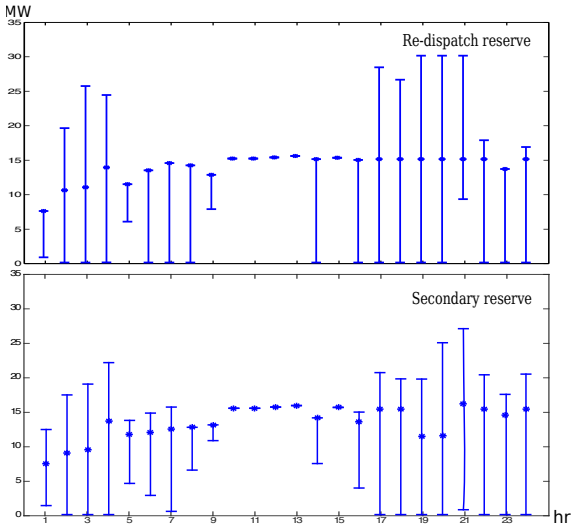

(a) Robust Approach

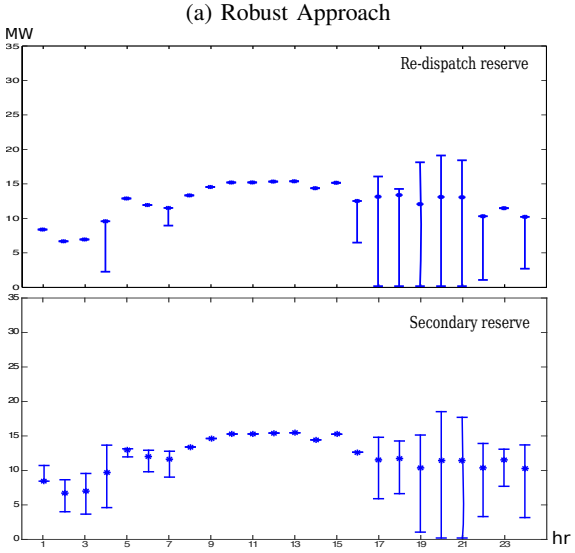

(b) Percentile Approach

Fig. 6: Generator Reserve Allocations (without ramp limits), for a single generator

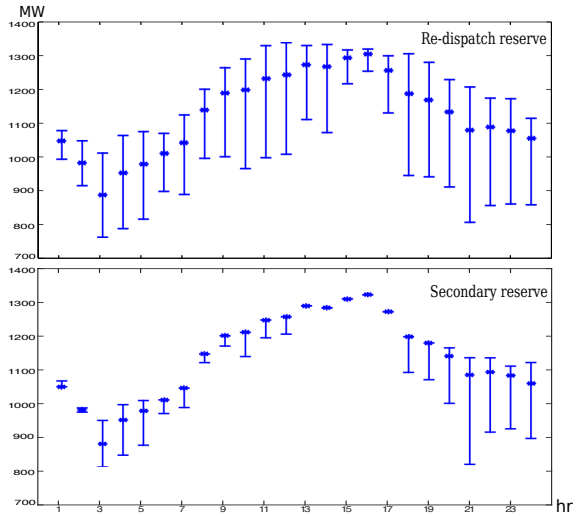

(a) Robust Approach

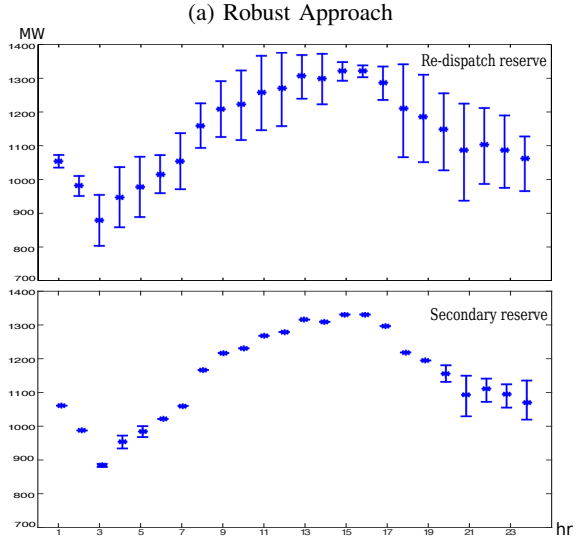

(b) Percentile Approach

Fig. 7: Total System Generation and Reserve Allocations (with ramp limits)

generator reserve requirements in the robust approach are significantly more than in the probabilistic solution. Invoking a robust approach for periods of highest uncertainty also exhibits this significant burden on the generators. In order to understand the infeasibility of the robust approach at higher levels of wind, Fig. 6 presents the reserve allocations for robust and probabilistic approaches with 30% wind, for a single bus. It is important to note that for this specific figure only, there are no ramp constraints in the model.

Examination of Fig. 6 illustrates the primary reason for infeasibility in robust solutions, where the dispatch point of the generator is indicated by the marker, and error bars provide up/down reserve allocations. Figure 6a shows a higher generator dispatch point, and greater demand for up/down reserves. Specifically, the downward reserves require the generator to immediately ramp down to zero output during many hours of the horizon. Inclusion of ramp limits in the constraint set of the optimization immediately creates infeasibilities in the solution. Conversely, this phenomenon very occasionally appears in the percentile approach from a lower dispatch point. Including ramp limits produces the system-wide reserve allocations shown in Fig. 7 which shows, not surprisingly, that greater reserves are allocated under the robust constraints, but the up/down reserves are now feasible in all cases.

In addition to the feasibility of different levels of wind share, the system cost of executing these solutions is an important metric for comparison. These results, shown in Fig. 8 illustrate that the increase in cost from 95% to the robust case (100%) is significant, and relatively large compared to that from 85% to 90% to 95%. The marginal cost of reliability is increasing as the solution approaches robustness, and the rate of this increases for higher levels of uncertainty.

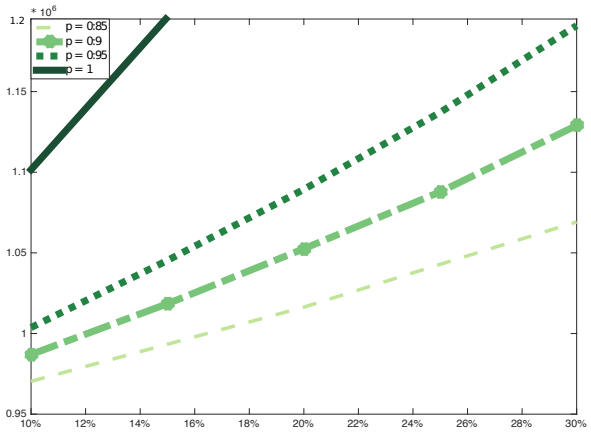

Fig. 8: Cost Comparison for 10% and 15% share of wind power.

IV. Concluding Remarks

This paper explored the effect of system flexibility, in terms of controllable loads and different risk levels, on the integration of significant wind resources within a chance-constrained unit commitment framework. Results have shown that the availability of reserves from controllable loads is effective in enabling higher wind integration levels, but that increasing controllable loads to a higher percentage of total load does not provide further benefits. This is a result of the type of loads in this study – the thermostatically controlled loads are realistically modeled with storage-like characteristics. The energy used from controllable loads for reserves must be returned to the system during the subsequent time period, thereby limiting the usefulness of additional reserves of this type. This finding leads to the conclusion that there is a need for responsive demand sources with different characteristics or costs, in addition to the controllable loads included in this study.

In addition, results show that the advantage of total reliability from robust solutions may not be synergistic with the societal goal of integrating significant uncertain renewable resources in the existing power system, due to its heavy burden on controllable generation. A more flexible solution, such as that provided by the chance-constrained formulation, can provide a middle ground between the deterministic-equivalent solution and the overly conservative robust solution. In addition to operational burden, the additional cost of robust solutions is significant over probabilistic solutions, even with high probability on the constraints.

While this simulation study has shown some interesting comparisons, and highlighted the importance of various classes of flexibility to wind integration, it also requires additional work to provide practical answers. Specifically, the controllable loads modeled here are a deterministic function of ambient temperature. It is widely acknowledged that demand response is not a deterministic resource [30]. Given the importance of this resource in the results presented here, it is clearly important to introduce uncertainty into the load side of this model, as was done in [19], [20], [31]. Also other classes of controllable loads will be explored in future explorations within this framework. Finally, the results presented here are specific to the 57-bus system. While many of these findings are likely universal, the usefulness of a unit commitment model is limited if it is not scalable to networks of practical size. Therefore, decomposition methods will be explored to allow the application to large networks.

References

[1] "Benefits of demand response in electricity markets and recommendations for achieving them," Department of Energy, Tech. Rep., February 2006. [Online]. Available: http://energy.gov/sites/prod/files/oeprod/DocumentsandMedia/DOE_Benefits_of_Demand_Response_in_Electricity_Markets_and_Recommendations_for_Achieving_Them_Report_to_Congress.pdf

[2] A. Faruqui, R. Hledik, S. George, J. Bode, P. Mangasarian, I. Rohmund, G. Wikler, D. Ghosh, and S. Yoshida, "A national assessment of demand response potential," Federal Energy Regulatory Commission, Tech. Rep., 2009. [Online]. Available: http://www.ferc.gov/legal/staff-reports/06-09-demand-response.pdf

[3] B. Bayer, "Current practice and thinking with integrating demand response for power system flexibility in the electricity markets in the usa and germany," *Current Sustainable/Renewable Energy Reports*, vol. 2, no. 2, pp. 55–62, 2015.

[4] A. Lamadrid, T. Mount, R. Zimmerman, C. Murillo-Sanchez, and C. L. Anderson, "Alternate mechanisms for integrating renewable sources of energy into electricity markets," *IEEE Power and Energy Society General Meeting*, June 2012.

[5] A. M. Gopstein, "Energy Storage and the Grid - From Characteristics to Impact [Point of View]," *Proceedings of the IEEE*, vol. 100, no. 2, pp. 311–316, June 2015.

[6] J. Cardell and C. L. Anderson, "A Flexible Dispatch Margin for Wind Integration," *IEEE Transactions on Power Systems*, pp. 1–8, May 2014.

[7] M. Albadi and E. El-Saadany, "Demand response in electricity markets: An overview," in *Power Engineering Society General Meeting, 2007. IEEE*, June 2007, pp. 1–5.

[8] C. Su and D. Kirschen, "Quantifying the effect of demand response on electricity markets," *Power Systems, IEEE Transactions on*, vol. 24, no. 3, pp. 1199–1207, 2009.

[9] N. Li, L. Chen, and S. Low, "Optimal demand response based on utility maximization in power networks," in *Power and Energy Society General Meeting, 2011 IEEE*, July 2011, pp. 1–8.

[10] M. Albadi and E. El-Saadany, "A summary of demand response in electricity markets," *Electric Power Systems Research*, vol. 78, no. 11, pp. 1989 – 1996, 2008. [Online]. Available: http://www.sciencedirect.com/science/article/pii/S0378779608001272

[11] N. O'Connell, P. Pinson, H. Madsen, and M. O'Malley, "Benefits and challenges of electrical demand response: A critical review," *Renewable and Sustainable Energy Reviews*, vol. 39, pp. 686 – 699, 2014. [Online]. Available: http://www.sciencedirect.com/science/article/pii/S1364032114005504

[12] F. Magnago, J. Alemany, and J. Lin, "Impact of demand response resources on unit commitment and dispatch in a day-ahead electricity market," *International Journal of Electrical Power & Energy Systems*, vol. 68, no. 0, pp. 142 – 149, 2015. [Online]. Available: http://www.sciencedirect.com/science/article/pii/S0142061514007625

[13] S. Madaeni and R. Sioshansi, "Measuring the benefits of delayed price-responsive demand in reducing wind-uncertainty costs," *Power Systems, IEEE Transactions on*, vol. 28, no. 4, pp. 4118–4126, Nov 2013.

[14] Y. Ikeda, T. Ikegami, K. Kataoka, and K. Ogimoto, "A unit commitment model with demand response for the integration of renewable energies," in *Power and Energy Society General Meeting, 2012 IEEE*, July 2012, pp. 1–7.

[15] A. Papavasiliou and S. Oren, "Large-scale integration of deferrable demand and renewable energy sources," *Power Systems, IEEE Transactions on*, vol. 29, no. 1, pp. 489–499, Jan 2014.

[16] H. Held, G. Martínez, and P. Steizig, "Stochastic programming approach for energy management in electric microgrids," *Numerical Algebra, Control and Optimization (NACO)*, vol. 4, no. 3, pp. 241–267, 9 2014, doi:10.3934/naco.2014.4.241.

[17] C. Zhao, J. Wang, J.-P. Watson, and Y. Guan, "Multi-stage robust unit commitment considering wind and demand response uncertainties," *Power Systems, IEEE Transactions on*, vol. 28, no. 3, pp. 2708–2717, Aug 2013.

[18] J. Aghaei and M. Alizadeh, "Robust $n-k$ contingency constrained unit commitment with ancillary service demand response program," *Generation, Transmission Distribution, IET*, vol. 8, no. 12, pp. 1928–1936, 2014.

[19] M. Vrakopoulou, J. Mathieu, and G. Andersson, "Stochastic Optimal Power Flow with Uncertain Reserves from Demand Response," in *Hawaii International Conference on System Sciences (HICSS)*, 2014, pp. 2353–2362.

[20] B. Li and J. Mathieu, "Analytical Reformulation of Chance-Constrained Optimal Power Flow with Uncertain Load Control," in *PowerTech*, Eindhoven, Netherlands, 2015.

[21] J. Liu, G. Martinez, B. Li, J. Mathieu, and C. L. Anderson, "A comparison of robust and probabilistic reliability for systems with renewables and responsive demand," *To appear in Proceedings of the 49th Hawaii Conference on System Sciences*, pp. 1–8, 2016.

[22] J. Mathieu, M. Kamgarpour, J. Lygeros, G. Andersson, and D. Callaway, "Arbitraging intraday wholesale energy market prices with aggregations of thermostatic loads," *IEEE Trans Power Systems*, vol. 30, no. 2, pp. 763–772, 2015.

[23] M. Vrakopoulou, K. Margellos, J. Lygeros, and G. Andersson, "Probablilistic guarantees for the N-1 security of systems with wind power generation," *International Conference on Probabilistic Methods Applied to Power System*, 2012.

[24] R. Zimmerman, C. Murillo-Sanchez, and R. Thomas, "Matpower's extensible optimal power flow architecture," in *Power Energy Society General Meeting, 2009. PES '09. IEEE*, July 2009, pp. 1–7.

[25] NREL, "Wind systems integration eastern wind integration and transmission study," National Renewable Energy Laboratory, Tech. Rep., 2010.

[26] C. L. Anderson and R. D. Zimmerman, "Wind Output Forecasts and Scenario Analysis for Stochastic Multiperiod Optimal Power Flow," in *PSERC Webinar*, Mar. 2011, pp. 1–38.

[27] K. Margellos, P. Goulart, and J. Lygeros, "On the road between robust optimization and the scenario approach for chance constrained optimization problems," *IEEE Transactions on Automatic Control*, vol. 59, no. 8, pp. 2258–2263, 2014.

[28] G. Martinez and C. L. Anderson, "A Risk-averse Optimization Model for Unit Commitment Problems," *Proceedings of the 48th Hawaii Conference on System Sciences*, pp. 1–9, 2015.

[29] P. Pinson, "Wind energy: Forecasting challenges for its operational management," *Statistical Science*, vol. 28, no. 4, pp. 564–585, 11 2013.

[30] J. Mathieu, M. González Vayá, and G. Andersson, "Uncertainty in the flexibility of aggregations of demand response resources," in *Proceedings of the IEEE Industrial Electronics Society Annual Conference*, Vienna, Austria, Nov. 2013.

[31] Y. Zhang, S. Shen, and J. Mathieu, "Data-driven optimization approaches for optimal power flow with uncertain reserves from load control," in *Proceedings of the American Control Conference (ACC)*, Chicago, IL, 2015.